

# Rhus Coriaria L. Ameliorates Gentamicin-Induced Nephrotoxicity in Diabetic Rats by Interference with LRP2 Receptor Expression and P53/TNF- $\alpha$ Downregulation

Original  
Article

Hend Ragab Mousa<sup>1</sup>, Lamiaa M. Shawky<sup>2</sup> and Ahmed A. Morsi<sup>3</sup>

<sup>1</sup>Department of Anatomy and Embryology, Faculty of Medicine, Benha University, Egypt

Department of Histology and Cell Biology, Faculty of Medicine, <sup>2</sup>Benha University, <sup>3</sup>Fayoum University, Egypt

## ABSTRACT

**Introduction:** An antidiabetic potential has long been reported for *Rhus coriaria* L. (sumac) and recent studies have proven a curative leverage against gentamicin (GM)-induced nephrotoxicity.

**Aim of the Work:** The current study hypothesized a possible Low-density lipoprotein-related receptor protein 2 (LRP2) expression modulatory effect, as an ameliorative mechanism, produced by sumac in GM-induced nephrotoxicity in diabetic rats.

**Material and Methods:** Forty-two male albino rats were subdivided into control, sumac alone (orally for 14 days), diabetes mellitus (DM, given single intravenous dose of streptozotocin (STZ), GM (intraperitoneal, once daily for 7 days), DM/GM, and DM/GM+sumac groups. Twenty-Four hrs after the last treatment, blood sampling was done for laboratory analysis of blood glucose, urea, and creatinine. The kidneys were harvested and subjected to RT-PCR quantification of LRP2 (megalin) mRNA levels, Hematoxylin and Eosin, Masson trichrome staining, and immunohistochemical assaying for P53, TNF- $\alpha$ , and megalin.

**Results:** Diabetic rats showed altered biochemical and histological findings which increased in the GM alone group and showed more serious tubular and glomerular injury in GM/DM group including disorganized glomeruli with mesangial degeneration and cellular depletion with hypertrophy of the remaining ones. The renal tubules were enlarged with sloughing and desquamation of the tubular lining cells. This was associated with significant elevation of the renal functions, upregulation of megalin gene/protein expression, in addition to increased P53 and tumor necrosis factor- $\alpha$  (TNF- $\alpha$ ). Sumac treatment downregulated megalin gene/protein expression, coupled with regulation of P53 and TNF- $\alpha$  expression and maintenance of the renal functions.

**Conclusion:** GM injection in already existing STZ-induced diabetic rats led to more serious renal damage, and sumac co-treatment protected against this renal damage, might be via LRP2 blockage dependent P53/TNF- $\alpha$  downregulation.

**Received:** 09 November 2022, **Accepted:** 04 December 2022

**Key Words:** Aminoglycoside renotoxicity, diabetic nephropathy, megalin.

**Corresponding Author:** Hend Ragab Mousa, MD, Department of Anatomy and Embryology, Benha Faculty of Medicine, Benha University, Egypt, **Tel.:** +20 12 2289 8035, **E-mail:** drhendragab@yahoo.com

**ISSN:** 1110-0559, Vol. 47, No. 1

## INTRODUCTION

Gentamicin (GM) belongs to the aminoglycoside class of antibiotics, and it has been cautiously prescribed in patients with gram-negative infections due to its oto/nephrotoxicity. However, it is still recommended for use in pediatric clinical practice to combat neonatal sepsis<sup>[1]</sup>. Moreover, GM has proven a paramount efficacy in carbapenem-resistant Enterobacteriaceae either alone or combined with other antibiotics<sup>[2]</sup>. All these clinical situations have obliged its increasing use, therefore searching for a solution to antagonize its organ toxicity is worthwhile.

Chronic diseases such as Diabetes Mellitus (DM) are identified as risk factors for acute renal injury in intensive care unit (ICU) patients or those under diagnostic procedures using nephrotoxic agents. Diabetic nephropathy is one of the most common long-run complications of DM. Hence, the urgency of GM use in diabetics could be a challenge facing physicians owing to the severe renal damage that will be added to the already ailing

kidneys of diabetic individuals. The paucity of recent data regarding the mechanisms of renal injury caused by GM, on a background of co-morbidities like diabetes has paid attention of the authors to investigate the co-existing of gentamicin toxicity in diabetic individuals<sup>[3,4]</sup>.

Low-density lipoprotein-related receptor protein 2 (LRP2), also called megalin, is a single trans-membrane protein that is normally expressed in the kidney, mainly, in proximal convoluted tubules (PCT). Extra-renal expressions include lungs, eye, gall bladder, and para/thyroid glands. Megalin is a multi-ligand receptor having the ability to bind many molecules (such as albumin, insulin, lipoproteins, and drugs such as gentamicin and polymyxin B) facilitating their endocytosis in the PCT<sup>[5,6]</sup>. The key element in gentamicin-induced nephrotoxicity is its entry and accumulation in the proximal tubules lining cells facilitated by receptor-mediated endocytosis, a selective transport pathway formed of megalin, cubilin, chloride channel-5 (CIC-5), and amnionless. After internalization, GM is transported to lysosomes leading to lysosomal accumulation, reactive oxygen species release, lysosomal

membrane permeabilization and lysosomal disruption followed by GM release into the cytoplasm with eventual tubular cell apoptosis<sup>[7,8]</sup>.

The protection against aminoglycosides-induced nephrotoxicity has been attempted in literature. One of the proposed approaches, antioxidants have proven marked efficacy against GM-induced renal toxicity, which may be owing to their capability to interfere with certain mechanistic aspects involved in such toxicity<sup>[9]</sup>. *Rhus coriaria* L., Authority Sumac, Family Anacardiaceae<sup>[10]</sup> is a well-known spice and native medicine that widely grows in Mediterranean countries, South Europe, and North Africa and it was used by the indigenous people for medicinal purposes<sup>[11]</sup>. Ethanobotanical and traditional uses included antiemetic, anti-diarrheal, anti-hemorrhagic, asthma curative, cardioprotective, and anal pile astringent effects, in addition to kidney diseases treatments, meanwhile pharmacological actions include antimicrobial, antimutagenic, antioxidant, anti-ischemic, hypoglycemic and hypolipidemic activities<sup>[12]</sup>.

The effect of sumac treatment on the GM-induced kidney toxicity, particularly, on a diabetic background has not been well-studied yet. The study hypothesized blockage of the tubular expression of LRP2 (megalin) receptor by sumac treatment in the current rat model of GM mediated nephrotoxicity on a background of STZ-induced diabetes. Also, the study aimed to evaluate such megalin blockage effect on P53 and TNF- $\alpha$  signaling pathways using biochemical and histological study.

## MATERIAL AND METHODS

### Drugs

Garamycin® ampoules (containing gentamicin sulfate, 80 mg/2ml) were purchased from Schering-Plough Pharmaceutical Company, Egypt.

### Preparation and characterization of *Rhus coriaria* (sumac) aqueous extract

Sumac fruits were purchased from a local spice market, Benha, Egypt. The dried whole sumac fruits were thoroughly triturated using a home grinder machine. Eighty grams of the plant powder was dispersed in distilled water (500 mL). The mixture was gently stirred and boiled (100 °C) for 20 minutes. After that, the extract was filtered, centrifuged (8000g for 10 min at room temperature), the collected supernatant underwent concentration in a rotary evaporator, lyophilized (freeze-dried at -51°C) to produce the crude yield (18.7 g)<sup>[13]</sup>. For animal use, the crude plant powder was reconstituted in distilled water to get the required concentration (600 mg/kg/d). The active ingredients found in higher concentrations in the sumac purchased from the Egyptian markets were o-cymene,  $\beta$ -ocimene, and limonene as reported by the analytical study conducted by the Egyptian researcher, Farag *et al.*<sup>[14]</sup> using SPME-GC-MS method.

### Induction and evaluation of diabetes

Freshly prepared streptozotocin (STZ) solution (in Na citrate, 0.1 mol/L, pH 4.5) was intravenously injected, at a dose of 60 mg/kg through the tail vein of fasted rats (12 hours). Three days after injection, blood samples were collected and checked for diabetes induction using a glucometer (Accu-Check; Roche Diagnostics, Benzberg, Germany). Animals with fasting blood glucose levels  $\geq$  250 mg/dl after 3 weeks (day 21) were included in the study<sup>[15]</sup>.

### Ethical considerations

All animal procedures and experimentation were performed in compliance with the guidelines of the Faculty of Veterinary Medicine, Benha University, Benha, Egypt, and conformed to the Guide for Care and Use of Laboratory Animals published by the US National Institutes of Health<sup>[16]</sup>. The protocol of the study was revised and approved by the local Research Ethics Committee at the Faculty of Medicine, Benha University, Benha, Egypt. Whenever possible, it was attempted to utilize the least statistically acceptable number of animals per group and to avoid or minimize animal pain, suffering, and distress.

### Animals and study design

The study was conducted on 42 Wistar male albino rats at (4-5 weeks, 160-180 g) purchased from the animal house, Faculty of Veterinary Medicine, Benha University, Egypt. The rats were group caged, three per cage, at an ambient temperature of  $23 \pm 2$  °C, kept under a daily 12-hours light/dark cycle, and were provided with the commercial pellet food and water ad libitum. The animals were randomly divided into 6 groups, 7 rats each. The experiment was conducted in the Research Lab, Faculty of Medicine, Benha University, Egypt. For acclimatization to the new laboratory conditions, a seven-day-adaptation period was allowed before the commencement of the experiment. The animal groups were illustrated in figure 1 and were distributed as follows:

**Control group:** The animals received the corresponding vehicle for each treatment in the same volume and the same duration. They received single intravenous (IV) saline injection once on day 0. On day 21 and for 14 consecutive days, oral distilled water (vehicle for sumac) was given. Intraperitoneal (i.p.) saline (vehicle for GM) injection was given once daily during the last 7 days of distilled water oral gavage (on day 28).

**Sumac alone-treated group:** received a single IV saline injection on day 0 followed by oral sumac (600 mg/kg) starting on day 21 and continued for 14 consecutive days. The dose of sumac was selected based on parallel literature studies on organ toxicities<sup>[17,18]</sup>. Intraperitoneal (i.p.) saline injection was given once daily during the last 7 days of oral sumac treatment (starting on day 28).

**Diabetic group:** received single intravenous (IV) STZ injection on day 0. On day 21, the rats received distilled

water oral gavage for 14 days. i.p. saline injection was given once daily during the last 7 days of distilled water oral gavage (on day 28).

Gentamicin alone-treated group: received a single IV saline injection on day 0 followed by distilled water oral gavage starting on day 21 and continued for 14 consecutive days. Gentamicin (100 mg/kg, i.p., for 7 days)<sup>[8]</sup> was given once daily during the last 7 days of distilled water oral gavage (starting on day 28).

Diabetic/gentamicin-treated group: the diabetic rats received oral distilled water on day 21 and for 14 consecutive days. i.p. gentamicin was given once daily during the last 7 days of distilled water treatment (on day 28).

Diabetic/gentamicin+sumac-treated group: the diabetic animals received oral sumac on day 21 for 14 consecutive days. i.p. gentamicin was given once daily during the last 7 days of oral sumac treatment (starting on day 28).

Groups	Duration of treatments	
	Day 0	Day 21 to Day 28
Control	Intravenous (IV) saline once	Oral distilled water + intraperitoneal (i.p.) saline
Sumac (SMC)	IV saline once	Oral sumac
Diabetic (DM)	IV streptozotocin (STZ) once	Oral distilled water + i.p. saline
Gentamicin(GM)	IV saline once	i.p. gentamicin
DM/GM	IV STZ once	i.p. gentamicin
DM/GM/SMC	IV STZ once	Oral sumac + i.p. gentamicin

**Fig. 1:** Animal grouping and duration of different treatments. D0: day 0, D21: day21, D28: day28, D35: day35, IV: intravenous, i.p.: intraperitoneal, STZ: streptozotocin.

### Collection of samples

At the end of the experiment, the rats were anesthetized. The left ventricle was punctured for blood sampling and later laboratory analysis of serum creatinine, BUN, and blood glucose. After that, the anesthetized animals were killed by cervical dislocation. The abdomen was opened via ventral incision and the kidneys were removed, the left one was refrigerated at -20 °C for later gene study, and the right one was fixed in 10 % formalin solution for 48 hrs.

### Renal functions and blood glucose levels

According to the manufacturer's instructions, the corresponding kits were used for the measurement of the serum creatinine according to the modified Jaffé method<sup>[19]</sup>. BUN was determined by the enzymatic method<sup>[20]</sup>. Blood glucose was measured using a glucometer and its corresponding blood tests strips (Accu-Check; Roche Diagnostics, Germany.)

### RT-PCR assay for quantitative analysis of LRP2/megalin gene expression

The collected kidney samples were well-homogenized till the renal tissues became invisible. Initial isolation of the total RNA followed by spectrophotometry measurement of the RNA concentration was done. After that, the real-time-PCR Master Mix kit (Applied Biosystems, Cat

No. 4440040) was used to convert mRNA into cDNA and the PCR reaction was evaluated by StepOneSystem (RQ Manager 1.2, software v 2.1, Applied Biosystem). The relative expression of the targeted gene (LRP2) was normalized to the mean critical threshold (CT) values of GAPDH (housekeeping gene) using the  $\Delta\Delta CT$  method<sup>[21]</sup>. For cDNA synthesis, the thermocycler was set at 45°C (15 min) followed by 95°C (for 5 min) for polymerase activation and reverse transcriptase inactivation<sup>[22]</sup>. For detection of the rat LRP2 transcripts, the forward primer was 5'-CCACCATTCCCTCGACCC-3' and the reverse primer was 5'-ACTTCCACCCTCATTTCTTGGT-3'. The forward primer for rat GAPDH was 5'-CCCTGTGCATGTTTCCATACG-3' and the reverse one was 5'-TGATCCCAACTAACTCGCT-3'.

### Histopathological study and immunohistochemistry

The formalin-fixed kidneys were prepared for paraffin microtechniques i.e. dehydrated in ascending concentrations of ethanol, xylene-cleared, infiltrated by, embedded in paraffin, and then sectioned. Five micron-thickness renal sections were cut and subjected to Hematoxylin and Eosin (H & E), Masson Trichrome staining<sup>[23]</sup>, and immunohistochemical assaying<sup>[24]</sup> for detection of P53, megalin, and TNF- $\alpha$  immunexpressions. All the used markers were rabbit polyclonal primary antibodies (Catalog #: ab131442, ab76969, and A11534 respectively). P53 and megalin were purchased from Abcam, Cambridge, United Kingdom while, TNF- $\alpha$  was from ABclonal Inc., Woburn, MA, USA. For antigen retrieval, the sections were boiled for 10 min in citrate buffer (Catalog #: AP9003-125, EpreDia, Thermo Fisher Scientific) at pH 6. After that and for 1 hour, the renal sections were incubated with the primary antibodies (at dilutions 1:100, 1:1000, and 1:200 for P53, megalin, and TNF- $\alpha$  respectively) in PBS. The detection system used for completing the immunoreaction was rabbit-specific kits (TP-015-HD, Lab Vision™, Thermo Fisher Scientific). A chromogen, 3,3-diaminobenzidine (DAB), and hematoxylin counterstaining were used. The positive reaction appeared as brownish cytoplasmic discoloration with apical membranous intensity (for megalin), positive nuclear (for P53), and cytoplasmic (for TNF- $\alpha$ ). The positive controls were rat spleen, mouse kidney, and human cancer lung for P53, megalin, and TNF- $\alpha$  re-spectively. Omitting the step of the primary antibody was done to prepare the negative control slides. Slide visualization and image photographing were performed in the Anatomy Department, Faculty of Medicine, Benha University, Egypt. For such purpose, Nikon Eclipse 80i upright microscope (Nikon Corporation, Japan) with a fitted digital camera, TouPCam™ Xcam full HD camera (TouPCam Europe, Ultramacro Ltd., UK) was used.

### Histomorphometric study

Image analysis was done by a third person who was an expert in the field, and unaware of the experimental groups to ensure a blind approach. ImageJ software (Java; NIH,

Bethesda, Maryland, USA)<sup>[25]</sup> was used for morphometric analysis of the photomicrographs captured at the same exposure conditions. The H & E-stained photomicrographs were utilized for histomorphometric measurements of the glomerular perimeter, cellularity, Bowman's space area, tubular perimeter, tubular degeneration, and loss of brush borders (BB). Degenerated tubules were identified by their necrotic/apoptotic cell lining. Renal tubules with lost BB included those with partial or complete absence of the apical BB. The immunoassay photomicrographs were used for evaluation of the area percent of P53, and TNF- $\alpha$  immunoreaction, in addition to the area percent and optical density of megalin immunoexpression. Trichrome stained was used to evaluate the area percent of collagen fiber deposition. Only rounded or nearly rounded glomeruli and renal tubules were included in the morphometric study. Using the counting tool, the number of nuclei was counted per glomerulus. At magnification x200, a total of ten glomeruli and ten PCT per section/group were used for analysis. For each antibody marker, at magnification x400, ten randomly captured immunostained photomicrographs were used for analysis. The same magnification was used for collagen fiber evaluation. Data were imported in an excel file, and subjected to statistical analysis.

### Statistical analysis

All collected data were subjected to statistical analysis using GraphPad Prism (GraphPad Software, Version 8 for windows, San Diego, California, USA). The results were presented as a mean  $\pm$  SD. One-way ANOVA was used to detect significance, followed by Tukey's test for comparison between the means of the study groups. Initially, a check of normality was performed using Kolmogorov-Smirnov test. Statistical significance was set at  $p < 0.05$ .

## RESULTS

### *Effect of Sumac treatment on the renal functions and blood glucose level*

Regarding blood glucose levels (Table 1), the biochemical analysis showed insignificant changes in GM and sumac alone-treated groups when compared to the control values. However, there was a significant increase ( $p < 0.05$ ) in both DM and DM/GM groups when compared to control group. DM/GM sumac co-treatment group demonstrated a significant reduction ( $p < 0.05$ ) in blood glucose when compared to the DM/GM group. The renal functions presented major changes in the study groups (Table 1). No statistical significance was present between sumac alone treatment and control. Both renal parameters (urea & creatinine) showed a significant rise ( $p < 0.05$ ) in DM, GM, and DM/GM groups when compared to the control. Interestingly, sumac co-treatment preserved ( $p < 0.05$ ) the renal functions.

### *Effect of sumac treatment on LRP2/megalyn gene expression*

LRP2 gene expression was identical with no statistical significance in both control and sumac alone-treated rats.

Both diabetic and gentamicin alone-treated animals show a significant rise ( $P < 0.05$ ) in LRP2 gene expression when compared to the control. A further significant increase ( $P < 0.05$ ) was noted in gentamicin-treated diabetic rats. On the other hand, sumac treatment in the latter group showed a significant decline ( $P < 0.05$ ) in LRP2 gene expression, in comparison to the gentamicin-treated diabetic animals (Figure 2).

### *Effect of sumac treatment on the renal histopathological changes induced by gentamicin in diabetic rats*

Light microscopic examination of the H&E-stained renal sections collected from both control (Figure 3a) and Sumac-treated (Figure 3b) groups displayed an identical normal histoarchitecture of the renal sections. Both groups showed the normal structure of the different segments of the nephron. The renal corpuscle was formed of Bowman's capsules (BC) surrounding capillary tufts "glomeruli". The parietal layer of the BC was lined by flat squamous cells and separated from the glomerulus by Bowman's space. The proximal convoluted tubules (PCT) appeared with a narrow uneven lumen and were lined by large pyramidal cells with rounded basal nuclei and acidophilic granular cytoplasm. The distal tubules (DCT) showed wide lumina with pale stained cuboidal lining cells.

In the diabetic group (Figure 4), the glomeruli were mainly affected. They showed mesangial expansion with thickening of the parietal layer of the BC. Mild glomerular congestion was noted. In addition, swollen tubular cells with vacuolar changes was seen among PCT. Eosinophilic substance deposits were frequently seen in Bowman's spaces and within the lumina of DCT.

In gentamicin-treated animals (Figure 5), the cortical architecture was disturbed. The renal glomeruli showed degenerated mesangial matrix with interglomerular empty spaces. Many renal corpuscles showed glomerular atrophy and widening of the renal spaces. The PCT appeared normalised with vacuolated cytoplasm and pyknotic nuclei. Marked interstitial vascular congestion was observed.

In DM/GT-treated group (Figure 6), marked affection of both glomerular and tubular hierarchies was evident. The glomeruli appeared necrotic, sloughed with degenerated vacuolated mesangium, and disappearing of some podocytes. The tubular lining cells looked sloughed and desquamated leaving denuded basal laminae. Nuclei were pyknotic.

On the opposite, the sumac co-treatment group (Figure 7) showed normal renal histological structure with seemingly intact glomeruli and renal tubules.

Masson trichrome-stained renal sections obtained from control (Figure 8a) and sumac-treated (Figure 8b) groups were similar and showed the typical distribution of collagen fibers with little interstitial collagen deposition and no fibrotic changes. In the diabetic group

(Figure 9c), the renal sections showed slight collagen deposition, peritubular, interglomerular (thick GBM), and brush borders which were more obvious and marked in the GM-treated group (Figure 9d). In DM/GM-treated group (Figure 10), there was a widespread greenish discoloration denoting diffuse collagen deposition. Meanwhile, the DM/GM sumac-cotreated group (Figure 11) showed an obvious reversal of fibrosis and maintenance of the normal distribution of collagen fibers.

### **Effect of Sumac treatment on the renal immunoeexpression of P53, TNF- $\alpha$ , and LRP2/Megalin**

Both control (Figure 12a) and sumac alone-treated (Figure 12b) groups showed identical findings. By comparison to the control group (Figure 12a), the results of P53 immunoreactivity showed few positive nuclei in the diabetic group (Figure 13c), increased gradually in the GM-treated group (Figure 13d), and became marked and widely distributed in DM/GM group (Figure 14). Regarding the TNF- $\alpha$  immunohistochemistry in the control (Figure 16a) and sumac (Figure 16b) groups, both groups showed consistent findings. Immunohistochemical observations of TNF- $\alpha$  displayed gradually increasing immunopositivity in DM (Figure 17c) and GM (Figure 17d) groups and became marked in DM/GM group (Figure 18). Megalin immunostaining revealed constitutive expression of megalin in the PCT of the control renal sections, mainly apical brush borders staining (Figure 20a), and similar expression was noted in sumac-treated group (Figure 20b), which mildly increased in the DM group (Figure 21), moderate expression in GM (Figure 22), and extremely expressed in DM/GM group (Figure 23). Meanwhile, the DM/GM sumac cotreated group displayed reversal and restoration of P53, TNF- $\alpha$ , and megalin immunoreactivities (Figures 15,19,24 respectively)

### **Effect of sumac co-treatment on the renal morphometric parameters**

The glomerular and tubular morphometric measurements were shown in (Table 2). Both control and sumac alone-treatment groups exhibited approximately equal glomerular parameters (equal renal capsular perimeter, Bowman's space (BS) area, and average cell number per glomerulus) with no statistical significance when compared to each other. The diabetic and GM groups showed a nonsignificant reduction in the capsular perimeter when compared to the control meanwhile, a significant reduction ( $p<0.05$ ) was noted in glomerular cellularity. However, the reduction in glomerular cellularity was slight in the diabetic group. In addition, the BS area was significantly reduced ( $p<0.05$ ) in the DM group and increased ( $p<0.05$ ) in GM alone group, indicating glomerular atrophy. Nevertheless, the DM/GM showed a significant decrease ( $p<0.05$ ) in the capsular perimeter, glomerular cellularity, and a significant increase ( $p<0.05$ ) in the BS area, all these parameters indicated shrinkage of the renal corpuscles and glomerular atrophy.

Regarding the tubular analysis (tubular perimeter, degeneration, loss of BB), no statistical significance existed when comparing both control and sumac alone-treatment groups. The diabetic group showed a significant increase ( $p<0.05$ ) in the tubular perimeter, number of degenerated tubules, and a mild significant increase in the number of tubules with lost BB when compared to control. In the GM group, there was a significant decrease ( $p<0.05$ ) in the tubular perimeter, in comparison to the control, but there was a statistically significant increase in the tubular degeneration and loss of BB. However, the DM/GM showed a significant increase ( $p<0.05$ ) in the atrophic tubules, tubular degeneration, and tubules ( $p<0.05$ ) with loss of the apical BB. Sumac co-treatment significantly improved ( $p<0.05$ ) both glomerular and tubular scoring parameters

The morphometric findings of the immunoassay slides were illustrated in (Figure 25). The area percent of P53, TNF- $\alpha$ , megalin immunoeexpressions, and trichrome-stained collagen fibers, in addition to the optical density of megalin immunopositivity, displayed no statistical significance in the sumac alone-treated group when compared to the control. All the measured parameters were significantly elevated ( $p<0.05$ ) in DM, GM, and DM/GM groups, in comparison to the control. A further significant rise ( $p<0.05$ ) was noticed in the DM/GM group when compared to DM or GM alone groups. GM alone group showed a significant rise ( $p<0.05$ ) in all these morphometric measurements (except area percent of collagen deposition) when compared to DM alone group. Sumac co-treatment significantly improved ( $p<0.05$ ) the disturbed measurements when compared to DM/GM group.

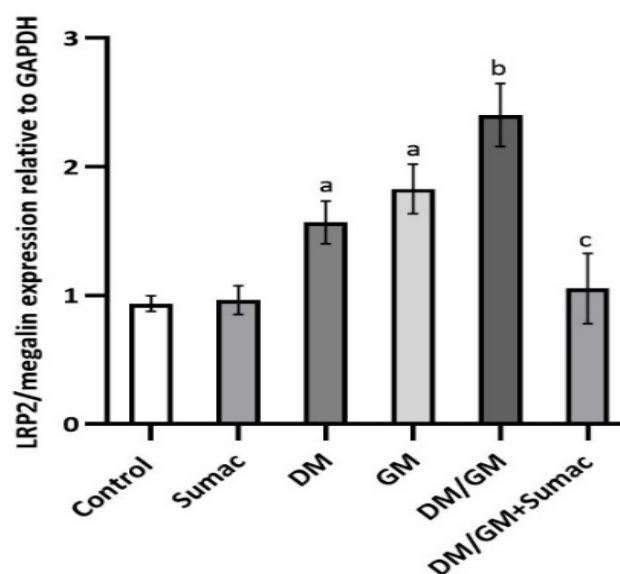


**Fig. 2:** Effect of sumac-cotreatment on LAR2/megalin gene expression. The data are expressed as mean  $\pm$  SD (n=7). a: significant versus control and sumac, b: significant versus DM and GM, c: sig-nificant versus DM/GM group, at  $p<0.05$ , using One-way ANOVA and post hoc Tukey's test

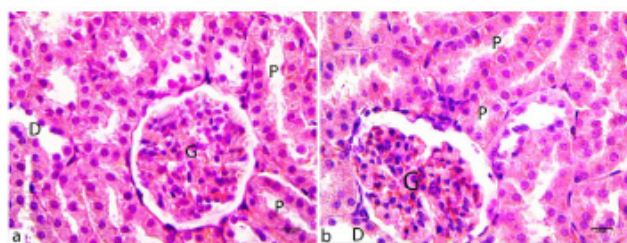


**Fig. 3:** H & E-stained photomicrographs of the control (a) and sumac-treated (b) groups renal (scale bar: 50  $\mu$ m) showing glomeruli (G) with normal cellularity, typical mesangial matrix, and average size. The PCT (P) looks with normal pyramidal cell lining. DCT (D) are also seen.

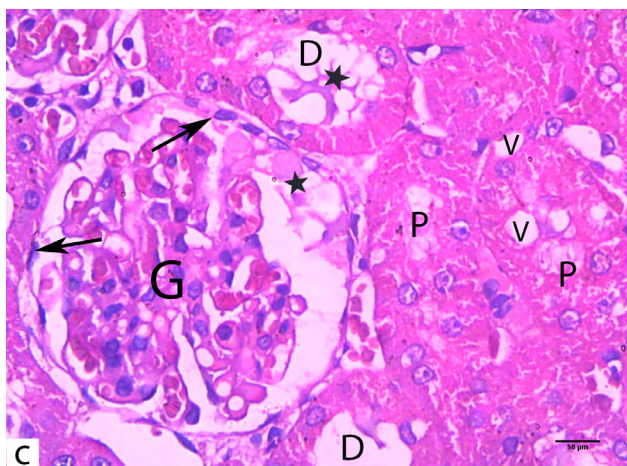


**Fig. 4:** H & E-stained photomicrograph of renal section in the diabetic group (scale bar: 50  $\mu$ m) showing glomeruli with mesangial proliferation and expansion, thickened parietal layer cell lining (arrows), and eosinophilic deposits in Bowman's space (star). The PCT (P) are dilated with swollen tubular cells and vacuolar changes (V). The DCT (D) shows luminal eosinophilic substance deposits (star).

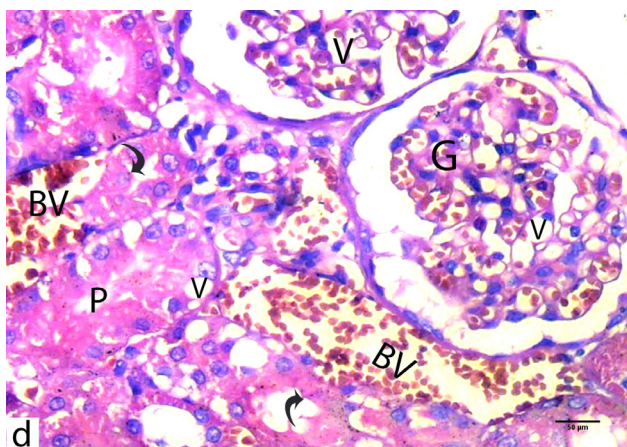


**Fig. 5:** H & E-stained photomicrograph of renal section in the gentamicin-treated group (scale bar: 50  $\mu$ m) showing marked interstitial vascular dilation and congestion (BV), and intraglomerular (G) mesangial degeneration with empty vacuolar changes (V). The PCT appears normal-sized with loss of the apical brush border (curved arrows) and vacuolated cytoplasm (V) of the lining cells.

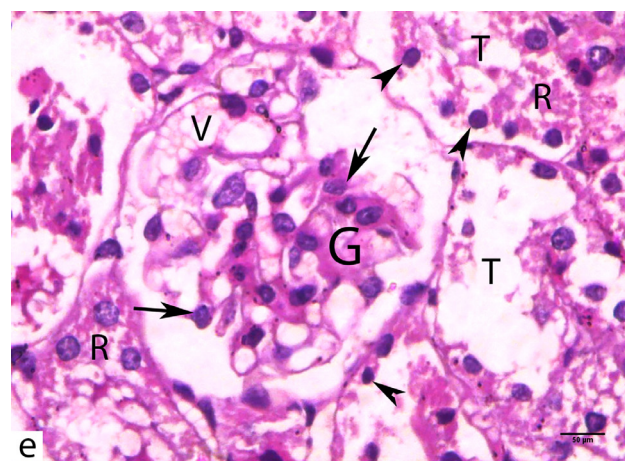


**Fig. 6:** H & E-stained photomicrograph of a renal section in the diabetes/gentamicin-treated group (scale bar: 50  $\mu$ m) showing marked glomerular and tubular injury. Glomeruli (G) appear disorganized with mesangial degeneration (V) and cellular depletion with hypertrophy of the remaining ones (arrows). The renal tubules (T) are dilated with sloughing and desquamation of the tubular lining cells, apoptotic nuclei (arrowheads), and cytoplasmic rarefaction (R).

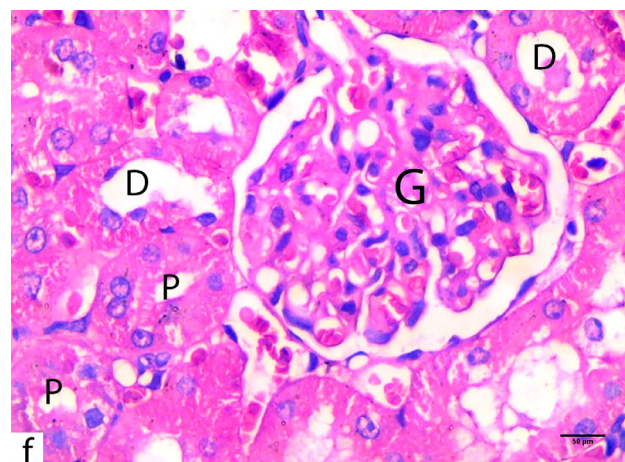


**Fig. 7:** H & E-stained photomicrograph of a renal section in the diabetes/gentamicin sumac co-treated group (scale bar: 50  $\mu$ m) showing restoration of the normal glomerular (G), proximal (P), and distal (D) tubular histological structure.

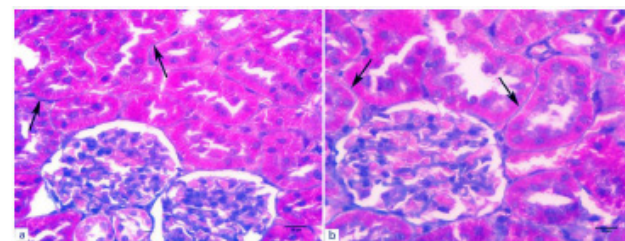


**Fig. 8:** Masson-stained photomicrographs of renal sections of both control (a) and sumac alone-treated (b) (scale bar: 50  $\mu$ m) showing the typical little density and distribution of the collagen fibers (green-stained) in-between renal tubules (arrows).

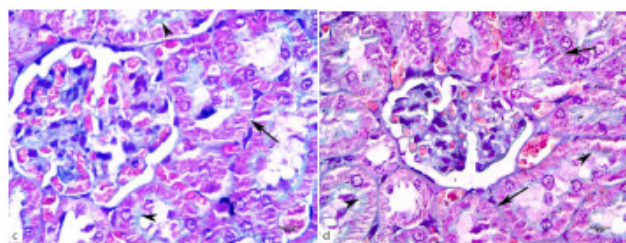


**Fig. 9:** Masson-stained photomicrographs of renal section in diabetic (c) and GM-treated (d) groups (scale bar: 50  $\mu$ m) showing collagen deposition in the tubular basal lamina (arrows) and brush borders (arrowheads) which markedly increased in the GM-treated group.

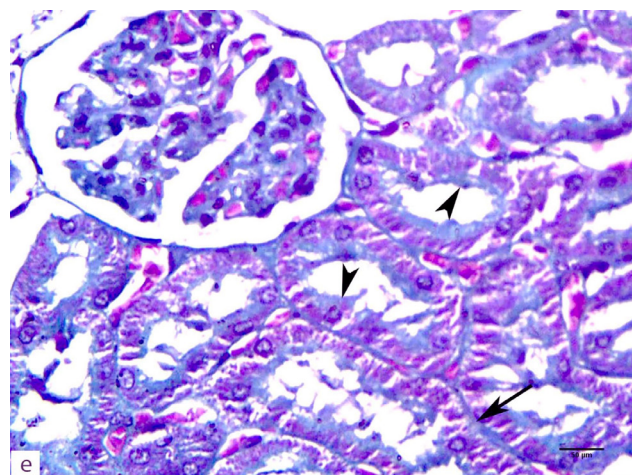


**Fig. 10:** Masson-stained photomicrographs of a renal section of DM/GM group (scale bar: 50  $\mu$ m) showing extensive and diffuse collagen deposition, peritubular (arrows), and apical brush borders (arrowheads).

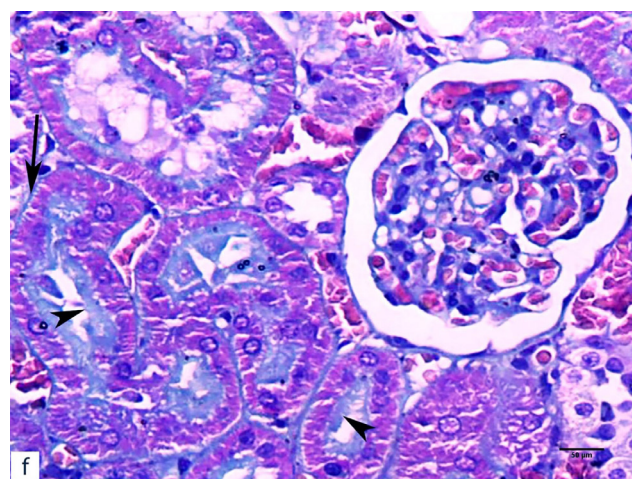


**Fig. 11:** Masson-stained photomicrographs of a renal section of the DM/GM sumac co-treated group (scale bar: 50  $\mu$ m) showing reversal of staining intensity indicating little collagen.

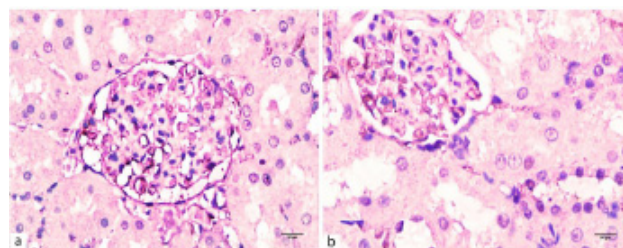


**Fig. 12:** Photomicrographs of P53 immunoassay renal sections in control (a) and sumac alone-treated (b) groups (scale bar: 50  $\mu$ m). The arrows refer to P53 positive nuclear reactions. Both groups show negative P53 immunoreaction.

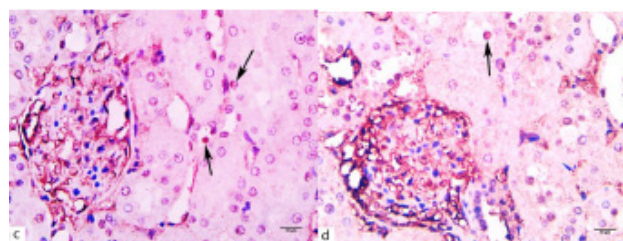


**Fig. 13:** Photomicrographs of P53 immunoassay renal section in diabetic (c) and GM-treated (d) groups (scale bar: 50  $\mu$ m) revealing very few positive nuclei, mildly increases in GM group.

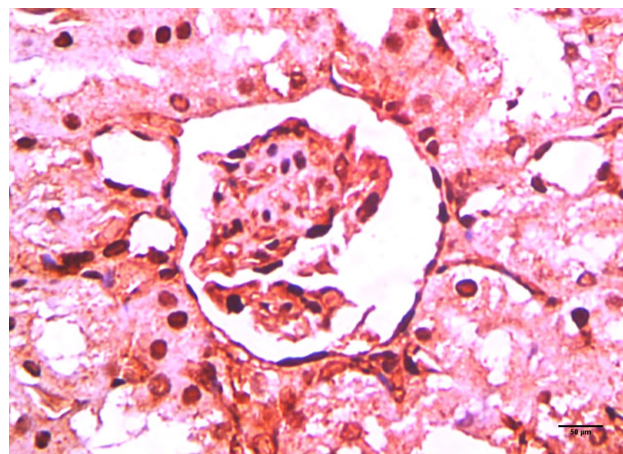


**Fig. 14:** Photomicrographs of P53 immunoassay a renal section in DM/GM group (scale bar: 50  $\mu$ m) revealing a marked diffuse positive nuclear reaction.

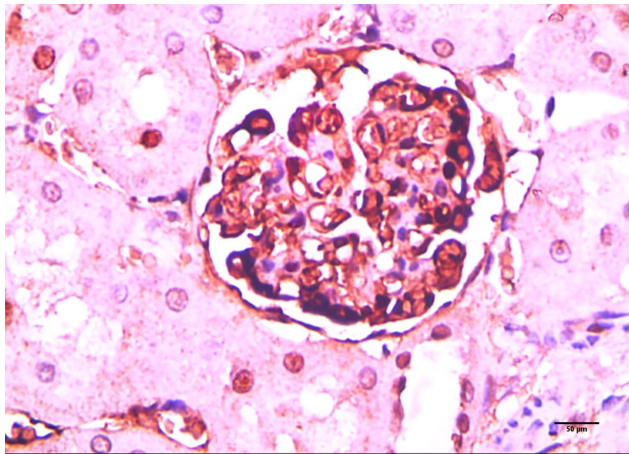


**Fig. 15:** Photomicrographs of P53 immunoassay a renal section in DM/GM sumac-cotreatment group (scale bar: 50  $\mu$ m) showing a less frequent positive nuclear reaction.

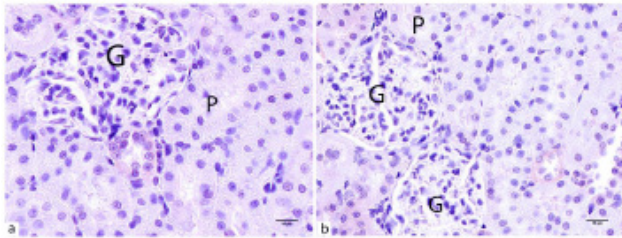


**Fig. 16:** Photomicrographs of TNF- $\alpha$  immunostained renal sections in control (a) and sumac alone-treated (b) groups (scale bar: 50  $\mu$ m) showing negative immunoreaction of the glomeruli (G) and proximal tubules (P).

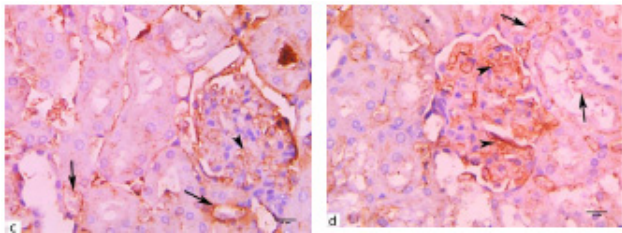


**Fig. 17:** Photomicrographs of TNF- $\alpha$  immunostained renal sections in diabetic (c) and GM-treated (d) groups (scale bar: 50  $\mu$ m) showing mild TNF- $\alpha$  cytoplasmic immunopositivity in the mesangial cells (arrowheads) and renal tubules (arrows) which gradually increases in the GM-treated group.

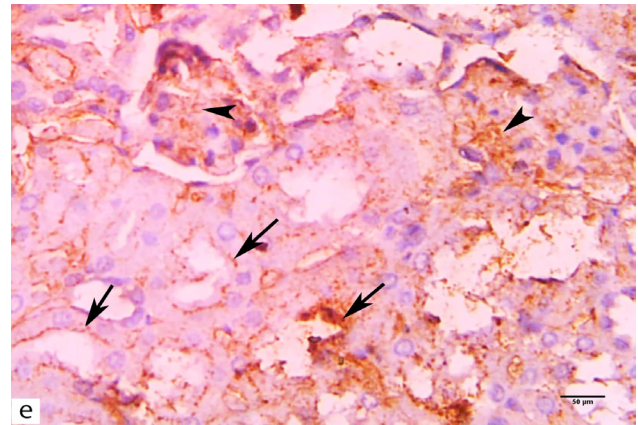


**Fig. 18:** Photomicrograph of TNF- $\alpha$  immunostained renal section in DM/GM group (scale bar: 50  $\mu$ m) showing marked expressed with a diffuse immunoreaction.

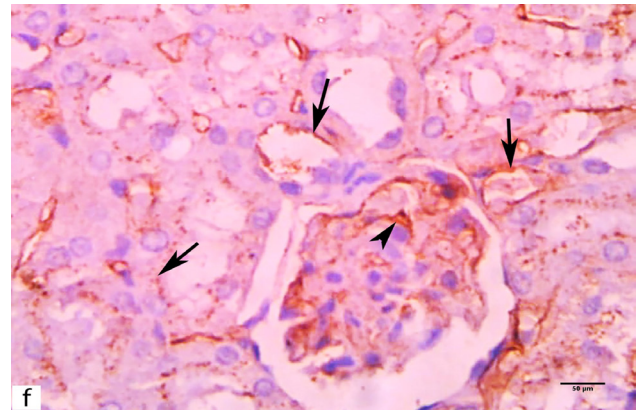


**Fig. 19:** Photomicrograph of TNF- $\alpha$  immunostained renal section in DM/GM sumac-cotreatment group (scale bar: 50  $\mu$ m) showing the mesangial cells (arrowheads) and renal tubules (arrows) with an obvious decrease in the TNF- $\alpha$  immunoreactivity.

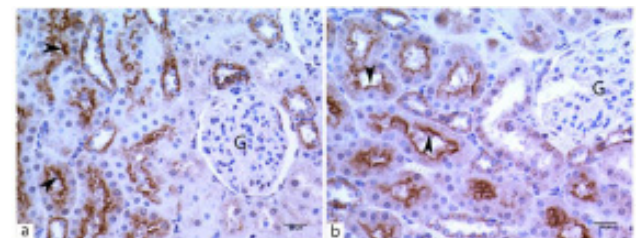


**Fig. 20:** Megalin (LRP2) immunoassayed photomicrographs of renal sections in both control (a) and sumac-treated (b) groups (scale bar: 100  $\mu$ m) showing megalin expression in renal tubules staining the apical brush borders (arrowheads) of proximal tubules. Glomeruli (G) show a negative reaction.



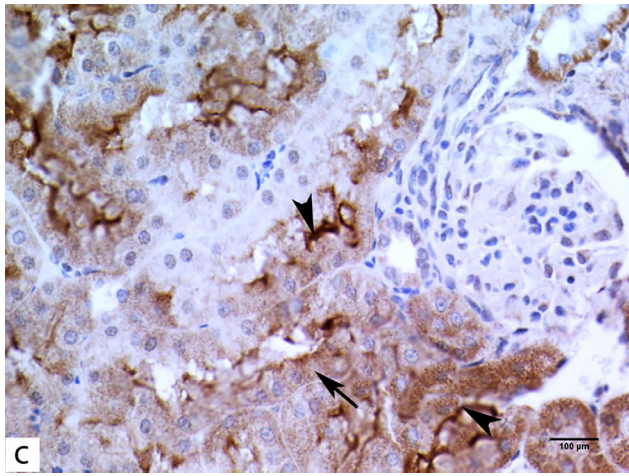


**Fig. 21:** Megalin (LRP2) immunoassayed photomicrograph in a renal section of diabetic group (scale bar: 100 μm) showing a mild increase in the tubular cytoplasmic (arrow) immunoreexpression and the apical brush border staining (arrowheads).

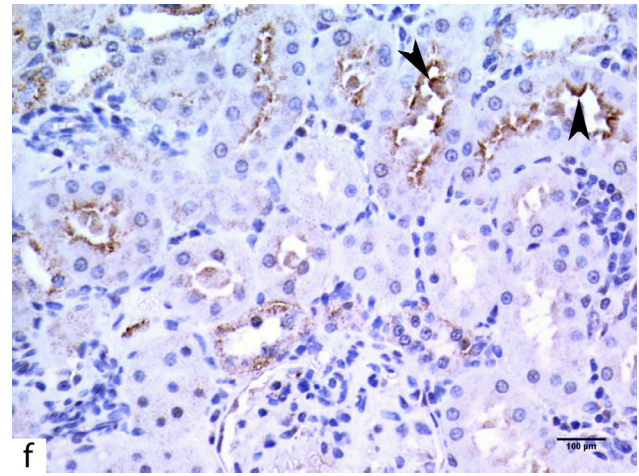


**Fig. 24:** Megalin (LRP2) immunoassayed photomicrograph in a renal section of DM/GM sumac co-treated group (scale bar: 100 μm) demonstrating a reversal of immunoreactivity with mild immunoreaction limited to apical brush borders (arrowheads).

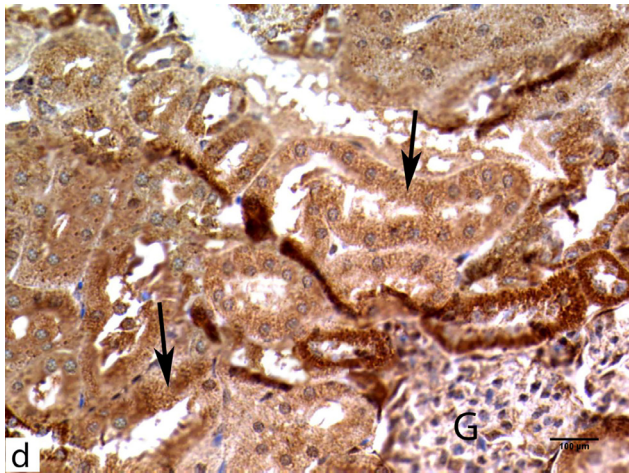


**Fig. 22:** Megalin (LRP2) immunoassayed photomicrograph in a renal section of GM-treated group (scale bar: 100 μm) showing diffuse moderate cytoplasmic expression (arrows).

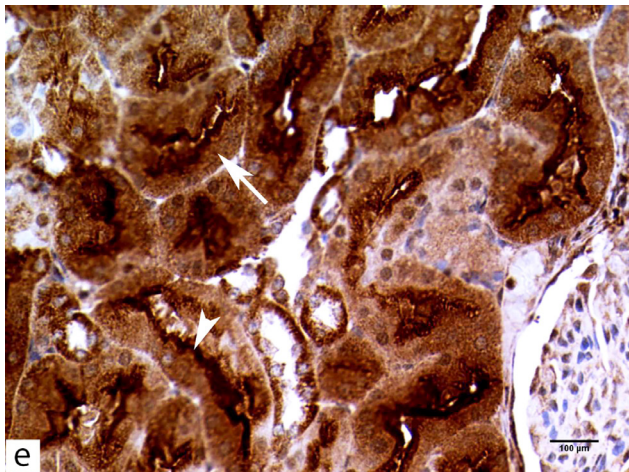


**Fig. 23:** Megalin (LRP2) immunoassayed photomicrograph in a renal section of DM/GM group (scale bar: 100 μm) exhibiting a diffuse strong positive cytoplasmic megalin immunopositivity (ar-row), in addition to dense apical brush border staining (arrowheads).

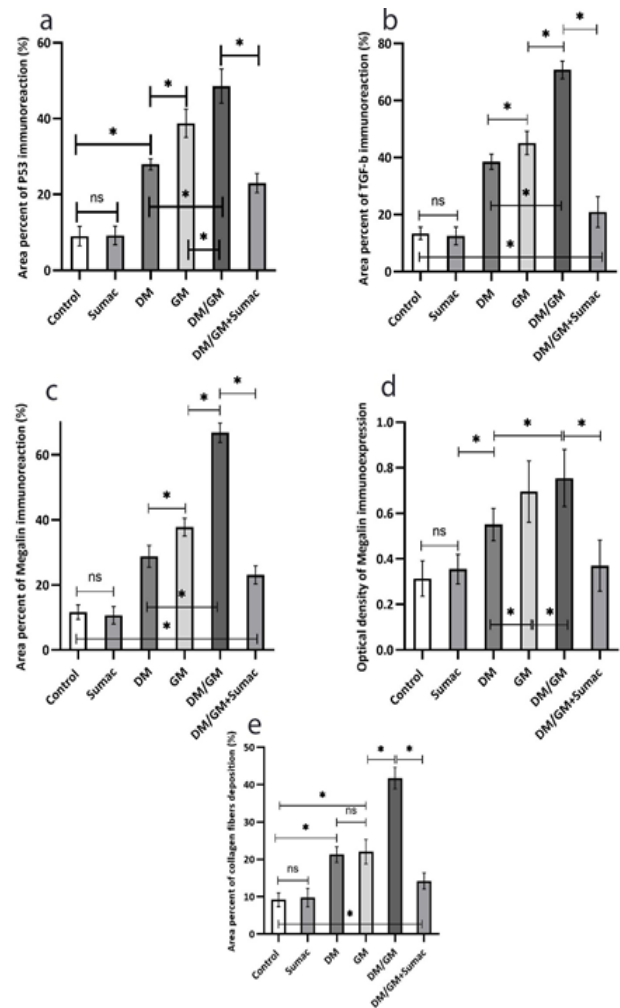


**Fig. 25:** Effect of sumac-cotreatment on the areas percent of P53 (a), TGF (b), Megalin (c) immunorepressions, trichrome stained collagen (e), and the optical density of megalin immunoreactivity (d). The data are expressed as mean ± SD (n=7). \* Statistically significant at p<0.05, using one-way ANOVA and post hoc Tukey's test.

**Table 1:** Changes in the renal functions and blood glucose levels under the effect of sumac co-treatment.

	Blood glucose (mg/dl)	S. creatinine (mg/dl)	BUN (mg/dl)
Control	93.2 ± 9.91	0.294 ± 0.11	28.46 ± 2.13
Sumac	94.25 ± 13.47	0.33 ± 0.13	28.68 ± 2.52
DM	344.8 ± 30.71 <sup>a</sup>	0.731 ± 0.17 <sup>a</sup>	36.25 ± 3.59 <sup>a</sup>
GM	97.98 ± 10.3	0.725 ± 0.1 <sup>a</sup>	37.54 ± 3.19 <sup>a</sup>
DM/GM	321.2 ± 22.73 <sup>a</sup>	1.01 ± 0.16 <sup>ab</sup>	46.67 ± 1.79 <sup>ab</sup>
DM/GM+Sumac	103.7 ± 7.68 <sup>c</sup>	0.388 ± 0.12 <sup>cd</sup>	29.8 ± 1.55 <sup>cd</sup>

The findings are presented as mean ± SD (n=7). Statistical significance was identified using one-way ANOVA followed by Post hoc Tukey's test for comparison between groups, at  $p < 0.05$ . <sup>a</sup> significant versus control. <sup>b</sup> significant versus DM & GM. <sup>c</sup> significant versus DM & DM/GM. <sup>d</sup> significant versus GM group.

**Table 2:** Changes in the glomerular and tubular parameters under the effect of sumac co-treatment during GM-induced nephrotoxicity in diabetic rats.

	Control	Sumac	DM	GM	DM/GM	DM/GM+Sumac
Capsular perimeter (um)	389.4 ± 19.17	389.9 ± 22.24	388.3 ± 15.37	366 ± 27.09	293.6 ± 8.89 <sup>a</sup>	382.8 ± 22.85
Glomerular cellularity	103.9 ± 16	102 ± 10.28	95.1 ± 7.46 <sup>a</sup>	87.2 ± 8.44 <sup>a</sup>	72.6 ± 11.66 <sup>c</sup>	102.5 ± 100 <sup>cd</sup>
Bowman space area (um <sup>2</sup> )	1895 ± 163.3	1927 ± 135.4	1476 ± 217 <sup>a</sup>	2631 ± 328.8 <sup>ab</sup>	3021 ± 108.5 <sup>c</sup>	1932 ± 149 <sup>cd</sup>
Tubular perimeter	183.3 ± 14.16	184.9 ± 11.77	246.1 ± 8.59 <sup>a</sup>	162.1 ± 10.69 <sup>ab</sup>	158 ± 10.4 <sup>c</sup>	174.7 ± 14.68 <sup>cd</sup>
Loss of brush border	0.5 ± 0.7	0.6 ± 0.69	1.2 ± 1.4 <sup>a</sup>	2.8 ± 1.5 <sup>ab</sup>	4 ± 1.56 <sup>c</sup>	0.7 ± 0.67 <sup>cd</sup>
Tubular degeneration	0.3 ± 0.4	0.4 ± 0.51	1 ± 0.67 <sup>a</sup>	2.2 ± 1.48 <sup>ab</sup>	3.3 ± 1.89 <sup>c</sup>	0.4 ± 0.52 <sup>cd</sup>

The findings are presented as mean ± SD (n=7). Statistical significance was identified using one-way ANOVA followed by Post hoc Tukey's test for comparison between groups, at  $p < 0.05$ . <sup>a</sup> significant versus control. <sup>b</sup> significant versus DM group. <sup>c</sup> significant versus DM & GM groups. <sup>d</sup> significant versus DM/GM groups, within the same row.

## DISCUSSION

The findings of the present study showed drastic changes in both renal functions and renal histological structure in gentamicin-intoxicated kidneys when induced on a background of diabetes. Also, the results showed an ameliorative effect of sumac co-treatment on such renal damage via anti-inflammatory, anti-apoptotic, antifibrotic, and megalin regulatory mechanisms.

The results of both control and sumac alone-treatment groups were identical regarding the biochemical, histological, and morphometric findings, so they were considered the same.

Streptozotocin-induced diabetic group showed glomerular affection in the H & E findings. Also, swollen tubular cells were evident. Further confirmation was reached via morphometric measurement of the glomerular and tubular parameters. Similarly, Feng *et al.*<sup>[26]</sup> reported slight significant parallel glomerular and tubular changes in STZ-mediated diabetes in rats. These histological changes were consistent with the significant elevation of BUN and creatinine in the same group. In the present study, the diabetic group displayed an increase in the area percent of TNF- $\alpha$  immunoreaction denoting renal inflammatory response. Also, there was a significant increase in the area percent of collagen deposition noticed in diabetic rats which might be explained by the increased TNF- $\alpha$  expression. Such an explanation might be in agreement with Taguchi *et al.*<sup>[27]</sup> who reported a therapeutic potential

for TNF- $\alpha$  inhibition on renal fibrosis and inflammation in aristolochic acid-induced mice nephropathy. Furthermore, the uncontrolled hyperglycemia triggered apoptotic changes as confirmed by the P53 positive tubular immunoreaction. This notion was supported by Zhong *et al.*<sup>[28]</sup> who reported Bax and caspase-9 mediated apoptosis elicited by the oxidative stress-induced hyperglycemia in diabetic nephropathy. Megalin is a specific marker of proximal convoluted tubules (PCT) being expressed in the cytoplasm and apical brush borders. It confers an endocytic pathway for gentamicin and other legends in PCT<sup>[5,6]</sup>. The current findings were in harmony with previous studies<sup>[29,30]</sup> which showed a significant increase in megalin expression in the early staged diabetic kidney. On the opposite, de Barros Peruchetti *et al.*<sup>[31]</sup> reported a suppression in megalin expression in LLC-PK1 (in *vitro* model of PCT cells) after 48 hrs incubation with high-glucose concentration.

Collectively, the upregulation of megalin gene/protein and TNF- $\alpha$  associated with the increase in P53 expression may highlight the histological characteristics of diabetic nephropathy in the diabetic group. The current suggestion was in alignment with the result of Romi *et al.*<sup>[7]</sup> who reported a substantial entanglement of megalin in renal apoptosis and tubular injury in diabetic rats.

In gentamicin alone-treatment group, the H&E findings referred to vacuolar degenerative changes in the tubular lining cells and glomerular mesangium. In accordance, Mohamed and Shenouda<sup>[9]</sup> reported both tubular and

glomerular affection in the same rat model of GM-induced renotoxicity. In addition, the results showed a statistically significant increase in the mean area percent of TNF- $\alpha$  immunoexpression which might be accused of the renal fibrosis induced in the same group and confirmed by the morphometric measurements of collagen fibers deposition. In consensus, Liu *et al.*<sup>[32]</sup> demonstrated that tubular injury could drive renal fibrosis and chronicity through the release of several mediators such as TNF- $\alpha$  from the tubular lining cells which, in turn, enhanced myofibroblast differentiation and proliferation.

In PCT, megalin receptor is committed for binding, entry, and accumulation of GM, where megalin is upregulated in GM-treated rats<sup>[8]</sup>. In agreement, the current finding showed a significant increase in the mean area percent of megalin immunoexpression in gentamicin-treated animals. Megalin-mediated endocytosis of GM leads to its storage and accumulation within lysosomes of PCT, lysosomal membrane breakage (due to phospholipidosis), the release of GM into cytoplasm, inflammation, and initiating apoptotic cell death<sup>[33]</sup>. In the same context, the results demonstrated a significant increase in the mean area percent of P53 when compared to the control confirming the activation of apoptotic signaling pathways. In harmony, Denamur *et al.*<sup>[34]</sup> reported a key regulatory role for P53 in apoptosis signaling pathway which was much expressed after GM exposure in renal cell lines.

On the other hand, gentamicin injection for 7 days in already diabetic rats (GM/DM group), resulted in radical changes in renal histoarchitecture with extreme glomerular and tubular affection coupled with altered renal functions. The authors suggested an exaggerated GM toxicity in already diabetic kidneys. The increased megalin expression in PCT of diabetic kidneys could facilitate further uptake and accumulation of GM in tubular lining cells, and hence more inflammation, and more apoptotic changes which were evident in the current findings of generous P53 and TNF- $\alpha$  immunostaining. The authors' suggestions bear a close resemblance to Hori *et al.*<sup>[35]</sup> who found that megalin receptor block by cilastatin could reduce GM-induced nephrotoxicity.

Recent animal models of combined gentamicin renotoxicity/diabetic nephropathy were scarce in the literature however, old studies<sup>[36,37]</sup> suggested a protective effect of DM against GM-induced nephrotoxicity due to decreased cellular uptake of GM in diabetic rats which was controversial to our findings.

Sumac (*Rhus coriaria*) plant is a well-recognized spice that has powerful antioxidant capabilities that make it worthy as a treatment modality in common diseases<sup>[38]</sup>. In the treatment group (GM/DM + sumac group), sumac co-treatment with gentamicin in diabetic rats showed a remarkable maintenance/restoration of the H&E and immunohistochemical findings of P53, TNF- $\alpha$ , in addition to downregulation of megalin gene/protein expression, and restoration of the renal functions, when compared to GM/

DM group. Due to the paucity of literature data, we believe that no other studies have evaluated sumac efficacy in gentamicin-induced renotoxicity on a background of STZ-induced diabetes. However, Doğan A, Çelik İ.<sup>[39]</sup> concluded a curative potential for sumac on STZ-induced rat diabetes and the associated diabetic nephropathy. Ghaznavi *et al.*<sup>[40]</sup> and Ahmadvand<sup>[41]</sup> reported a renoprotective effect of gallic acid (a sumac constituent), in GM-induced renal toxicity, via anti-inflammatory and anti-oxidative stress actions. Nevertheless, one limitation in the current study, that we would address in future research, was to investigate the antibacterial efficacy of gentamicin when combined with sumac.

## CONCLUSION

In the present study, STZ-induced diabetic animals showed an altered renal histoarchitecture. GM alone treatment resulted in disturbed biochemical, histological, and immunohistochemical findings. Gentamicin injections for 7 days in diabetic rats showed marked worsening of the renal functions, histological findings, and extreme inflammatory, fibrotic, and apoptotic changes. Nevertheless, sumac co-treatment was found to maintain and protect against GM-induced toxicity in diabetic rats via anti-inflammatory, antifibrotic, anti-apoptotic mechanisms facilitated by LRP2 (megalin) regulatory effects induced by sumac.

Taken together, the authors reported a directly proportional relationship between LRP2 gene/protein expression and P53/TNF- $\alpha$  upregulation. We observed little LRP2 expression in diabetic-only rats which increased gradually in gentamicin-only treated rats and became maximum in gentamicin-treated diabetic rats, then reversed after sumac treatment. P53 and TNF upregulation showed a proportional change in the same group sequence. This could imply LRP2/megalin-dependent P53 and TNF signaling in the current rat model. Therefore, the study presents an innovative modality or alternative for persons at risk for GM nephrotoxicity such as diabetic individuals.

## CONFLICT OF INTERESTS

There are no conflicts of interest.

## REFERENCES

1. Keerthana Chandrasekar VB, Vijay V, Shalini R, Arun KP. Gentamicin pharmacokinetics and pharmacodynamic correlation in pediatrics—A systematic review. *J Appl Pharm Sci* 2021; 11:11–17. DOI: 10.7324/JAPS.2021.1101102
2. Park SY, Lee JS, Oh J, Lee SH, Jung J. Effectiveness of selective digestive decolonization therapy using oral gentamicin for eradication of carbapenem-resistant Enterobacteriaceae carriage. *Infect Control Hosp Epidemiol* 2022:1–6. DOI: <https://doi.org/10.1017/ice.2021.492>

3. Martins ALC de L, Watanabe M, Fernandes SM, Fonseca CD da, Vattimo M de FF. Diabetes Mellitus: a risk factor for drug toxicity. *Rev Da Esc Enferm Da USP* 2018; 52:1–7. DOI: <https://doi.org/10.1590/s1980-220x2017033503347>
4. Mezil SA, Abed BA. Complication of diabetes mellitus. *Ann Rom Soc Cell Biol* 2021; 25:1546–1556. DOI: <https://doi.org/10.3390/2Fnu15030564>
5. Hirano M. An Endocytic Receptor, Megalin-Ligand Interactions: Effects of Glycosylation. *Trends Glycosci Glycotechnol* 2018; 30:E155–E160. DOI: 10.4052/tigg.1752.1E
6. Sun Y, Lu X, Danser AH. Megalin: a novel determinant of renin-angiotensin system activity in the kidney? *Curr Hypertens Rep* 2020; 22:1–7. doi: 10.1007/s11906-020-01037-1
7. Romi MM, Anggorowati N, Maulida DS, Suskalanggeng M, Setyaningsih WAW, Sari DCR, Arfian N. Upregulation of Megalin, Cubilin, NGAL mRNA expression in kidney may represent tubular injury and apoptosis in chronic condition of rat diabetic model. *Med J Malaysia* 2021; 76:87–92. PMID: 33510115
8. Azouz AA, Hanna DA, Abo-Saif AA, Messiha BAS. Interference with megalin expression/endocytic function by montelukast mitigates gentamicin nephrotoxicity: Downregulation of CIC-5 expression. *Saudi Pharm J* 2022; 30:150–161. DOI: <https://doi.org/10.1016/j.jsps.2021.12.013>
9. Mohamed HZE, Shenouda MBK. Amelioration of renal cortex histological alterations by aqueous garlic extract in gentamicin induced renal toxicity in albino rats: a histological and immunohistochemical study. *Alexandria J Med* 2021; 57:28–37. DOI: 10.1080/20905068.2020.1871179
10. Sağlam M, Köseoğlu S, Hatipoğlu M, Esen HH, Köksal E. Effect of sumac extract on serum oxidative status, RANKL/OPG system and alveolar bone loss in experimental periodontitis in rats. *J Appl Oral Sci* 2015; 23:33–41. DOI: <https://doi.org/10.1590/2F1678-775720140288>
11. Diler Ö, Özil Ö, Bayrak H, Yiğit NÖ, Özmen Ö, Saygın M, Aslankoç R. Effect of dietary supplementation of sumac fruit powder (*Rhus coriaria* L.) on growth performance, serum biochemistry, intestinal morphology and antioxidant capacity of rainbow trout (*Oncorhynchus mykiss*, Walbaum). *Anim Feed Sci Technol* 2021; 278:114993. DOI <https://doi.org/10.1590/1678-775720140288>
12. Abdul-Jalil TZ. *Rhus coriaria* (Sumac): A Magical Spice. *Herbs and Spices*. IntechOpen; 2020:39. DOI: 10.5772/intechopen.92676
13. Gabr SA, Alghadir AH. Evaluation of the biological effects of lyophilized hydrophilic extract of *Rhus coriaria* on myeloperoxidase (MPO) activity, wound healing, and microbial infections of skin wound tissues. *Evidence-Based Complement Altern Med* 2019; 2019. DOI: <https://doi.org/10.1155/2019/5861537>
14. Farag MA, Fayek NM, Abou Reidah I. Volatile profiling in *Rhus coriaria* fruit (sumac) from three different geographical origins and upon roasting as analyzed via solid-phase microextraction. *PeerJ* 2018; 6:e5121. DOI: <https://doi.org/10.7717/peerj.5121>
15. Shawky LM, Bana EA El, Morsi AA. Stem cells and metformin synergistically promote healing in experimentally induced cutaneous wound injury in diabetic rats. *Folia Histochem Cytobiol* 2019; 57:127–138. DOI: <https://doi.org/10.5603/fhc.a2019.0014>
16. NIH. *Guide for the Care and Use of Laboratory Animals*. 8th ed. New York, USA: National Academies Press (US); 2011. DOI: <http://dx.crossref.org/10.17226/12910>
17. Wu Z, Zhang Y, Gong X, Cheng G, Pu S, Cai S. The preventive effect of phenolic-rich extracts from Chinese sumac fruits against nonalcoholic fatty liver disease in rats induced by a high-fat diet. *Food Funct* 2020; 11:799–812. DOI: <https://doi.org/10.1039/C9FO02262G>
18. Wu Z, Ma Q, Cai S, Sun Y, Zhang Y, Yi J. *Rhus chinensis* Mill. Fruits Ameliorate Hepatic Glycolipid Metabolism Disorder in Rats Induced by High Fat/High Sugar Diet. *Nutrients* 2021; 13:4480. DOI: <https://doi.org/10.3390/2Fnu13124480>
19. Junge W, Wilke B, Halabi A, Klein G. Determination of reference intervals for serum creatinine, creatinine excretion and creatinine clearance with an enzymatic and a modified Jaffe method. *Clin Chim Acta* 2004; 344:137–148. DOI: <https://doi.org/10.1016/j.cccn.2004.02.007>
20. Manoukian E, Fawaz G. The enzymatic microestimation of urea 1969. DOI: <https://doi.org/10.1515/cclm.1969.7.1.32>
21. Livak KJ, Schmittgen TD. Analysis of relative gene expression data using real-time quantitative PCR and the 2<sup>-</sup>ΔΔCT method. *Methods* 2001; 25:402–408. DOI: <https://doi.org/10.1006/meth.2001.1262>
22. Tataurov A V, You Y, Owczarzy R. Predicting ultraviolet spectrum of single stranded and double stranded deoxyribonucleic acids. *Biophys Chem* 2008; 133:66–70. DOI: <https://doi.org/10.1016/j.bpc.2007.12.004>
23. Bancroft JD, Layton C. The Hematoxylin and Eosin /Connective and other mesenchymal tissues with their stains. In: Suvarna KS, Layton C, Bancroft JD (eds.), *Bancroft's theory and practice of histological techniques E-Book*. 8th ed. Elsevier Health Sciences; 2019. DOI: <https://doi.org/10.1016/B978-0-7020-4226-3.00010-X>

24. Kiernan JA. Immunohistochemistry. In: Kiernan J (ed.), *Histological and histochemical methods. Theory and practice*. 4th-th ed. Scion Publishing Ltd; 2015:454–490. DOI: <https://doi.org/10.4081%2Fejh.2016.2639>
25. Rasband WS. ImageJ; US National Institutes of Health: Bethesda, MD, 1997-2007. World Wide Web (<Http://Rsb Info Nih Gov/Ij/>) 2007. DOI: <https://doi.org/10.1038%2Fnmeth.2089>
26. Feng Y-Z, Chen X-Q, Cheng Z-Y, Lin Q-T, Chen P-K, Si-Tu D-K, Cao R, Qian L, Heng B, Cai X-R. Non-invasive investigation of early kidney damage in streptozotocin-induced diabetic rats by intravoxel incoherent motion diffusion-weighted (IVIM) MRI. *BMC Nephrol* 2021; 22:1–12. DOI: <https://doi.org/10.1186/s12882-021-02530-8>
27. Taguchi S, Azushima K, Yamaji T, Urate S, Suzuki T, Abe E, Tanaka S, Tsukamoto S, Kamimura D, Kinguchi S. Effects of tumor necrosis factor- $\alpha$  inhibition on kidney fibrosis and inflammation in a mouse model of aristolochic acid nephropathy. *Sci Rep* 2021; 11:1–11. DOI: <https://doi.org/10.1038/s41598-021-02864-1>
28. Zhong Y, Luo R, Liu Q, Zhu J, Lei M, Liang X, Wang X, Peng X. Jujuboside A ameliorates high fat diet and streptozotocin induced diabetic nephropathy via suppressing oxidative stress, apoptosis, and enhancing autophagy. *Food Chem Toxicol* 2022; 159:112697. DOI: <https://doi.org/10.1016/j.ftc.2021.112697>
29. Bryniarski MA, Yee BM, Jaffri I, Chaves LD, Yu JA, Guan X, Ghavam N, Yacoub R, Morris ME. Increased megalin expression in early type 2 diabetes: role of insulin-signaling pathways. *Am J Physiol Physiol* 2018; 315:F1191–F1207. DOI: <https://doi.org/10.1152/ajprenal.00210.2018>
30. Haraguchi R, Kohara Y, Matsubayashi K, Kitazawa R, Kitazawa S. New insights into the pathogenesis of diabetic nephropathy: proximal renal tubules are primary target of oxidative stress in diabetic kidney. *Acta Histochem Cytochem* 2020; 53:21–31. DOI: <https://doi.org/10.1267%2Fahc.20008>
31. de Barros Peruchetti D, Silva-Aguiar RP, Siqueira GM, Dias WB, Caruso-Neves C. High glucose reduces megalin-mediated albumin endocytosis in renal proximal tubule cells through protein kinase B O-GlcNAcylation. *J Biol Chem* 2018; 293:11388–11400. DOI: <https://doi.org/10.1074/jbc.ra117.001337>
32. Liu B-C, Tang T-T, Lv L-L. How tubular epithelial cell injury contributes to renal fibrosis. In: Liu B-C, Lan H-Y, Lv L-L (eds.), *Renal fibrosis: mechanisms and therapies*. 2019th ed. Springer; 2019:233–252. DOI: <https://doi.org/10.1038%2Fs41419-018-1157-x>
33. Nagai J, Takano M. Entry of aminoglycosides into renal tubular epithelial cells via endocytosis-dependent and endocytosis-independent pathways. *Biochem Pharmacol* 2014; 90:331–337. DOI: <https://doi.org/10.1016/j.bcp.2014.05.018>
34. Denamur S, Boland L, Beyaert M, Verstraeten SL, Fillet M, Tulkens PM, Bontemps F, Mingeot-Leclercq M-P. Subcellular mechanisms involved in apoptosis induced by aminoglycoside antibiotics: Insights on p53, proteasome and endoplasmic reticulum. *Toxicol Appl Pharmacol* 2016; 309:24–36. DOI: [10.1016/j.taap.2016.08.020](https://doi.org/10.1016/j.taap.2016.08.020)
35. Hori Y, Aoki N, Kuwahara S, Hosojima M, Kaseda R, Goto S, Iida T, De S, Kabasawa H, Kaneko R. Megalin blockade with cilastatin suppresses drug-induced nephrotoxicity. *J Am Soc Nephrol* 2017; 28:1783–1791. DOI: <https://doi.org/10.1681%2FASN.2016060606>
36. Teixeira RB, Kelley J, Alpert H, Pardo V, Vaamonde CA. Complete protection from gentamicin-induced acute renal failure in the diabetes mellitus rat. *Kidney Int* 1982; 21:600–612. DOI: <https://doi.org/10.1038/ki.1982.67>
37. Gouvea W, Vaamonde CM, Owens B, Alpert H, Pardo V, Vaamonde CA. The protection against gentamicin nephrotoxicity in the streptozotocin-induced diabetic rat is not related to gender. *Life Sci* 1992; 51:1747–1758. DOI: <https://doi.org/10.1038/ki.1982.67>
38. Alsamri H, Athamneh K, Pintus G, Eid AH, Iratni R. Pharmacological and antioxidant activities of *Rhus coriaria* L.(Sumac). *Antioxidants* 2021; 10:73. DOI: <https://doi.org/10.3390/antiox10010073>
39. Doğan A, Çelik İ. Healing effects of sumac (*Rhus coriaria*) in streptozotocin-induced diabetic rats. *Pharm Biol* 2016; 54:2092–2102. DOI: <https://doi.org/10.3109/13880209.2016.1145702>
40. Ghaznavi H, Fatemi I, Kalantari H, Hosseini Tabatabaei SMT, Mehrabani M, Gholamine B, Kalantar M, Mehrzadi S, Goudarzi M. Ameliorative effects of gallic acid on gentamicin-induced nephrotoxicity in rats. *J Asian Nat Prod Res* 2018; 20:1182–1193. DOI: <https://doi.org/10.1080/10286020.2017.1384819>
41. Ahmadvand H, Nouryazdan N, Nasri M, Adibhesami G, Babaenezhad E. Renoprotective Effects of Gallic Acid Against Gentamicin Nephrotoxicity Through Amelioration of Oxidative Stress in Rats. *Brazilian Arch Biol Technol* 2020; 63. DOI: <https://doi.org/10.1590/1678-4324-2020200131>

## الملخص العربي

يحسن نبات السماق من السمية الكلوية المستحثة بعقار الجنتاميسين في ذكور الجرذان البيضاء المصابة بمرض السكري من خلال اعتراض ظهور مستقبلات الـ " ال. ار. بي. ٢ " وتقليل مسار الـ " بي ٥٣ / تي. ان. اف- الفا

هند رجب موسى<sup>١</sup>، لمياء محمد شوقي<sup>٢</sup>، أحمد مرسي<sup>٣</sup>

قسم التشريح وعلم الأجنة، كلية الطب، جامعة بنها، مصر

قسم الأنسجة وبيولوجيا الخلية، كلية الطب، جامعة بنها، جامعة الفيوم، مصر

**المقدمة:** لقد تم الكشف منذ فترة طويلة عن وجود خصائص مضادة لمرض السكري في نبات السماق، وقد أثبتت الدراسات الحديثة وجود تأثير علاجي ضد السمية الكلوية المستحثة بدواء الجنتاميسين.

**الهدف من البحث:** افترضت الدراسة الحالية احتمالية وجود تأثير منظم لظهور الـ ال. ار. بي. ٢، كآلية تحسن، يقوم به السماق في السمية الكلوية المستحثة بعقار الجنتاميسين في الجرذان المصابة بداء السكري.

**المواد والطرق المستخدمة:** تم تقسيم اثنين وأربعين من ذكور الجرذان البيضاء إلى مجموعة تحكم، مجموعة السماق (عن طريق الفم لمدة ١٤ يومًا)، مجموعة مرض السكري المستحث بمادة السترينبتوزوتوسين، مجموعة الجنتاميسين فقط عن طريق الحقن البيروتوني مرة واحدة يوميًا لمدة ٧ أيام، مجموعة السكري والجنتاميسين، مجموعة السكري والجنتاميسين المعالجة بالسماق. تم أخذ عينات الدم للتحليل المعملية لنسبة الجلوكوز واليوريا والكرياتينين في الدم، وذلك بعد أربع وعشرون ساعة من اخر جرعة تم اعطائها. تم استئصال الكلى وإخضاعها لاختبار بي سي ار للتحديد الكمي لمستوي جين الميجالين، والهيماتوكسيلين والأيوسين، ماسون ثلاثي الكروم، والكشف عن بروتينات الـ بي 53 و تي. ان. اف- الفا، والميجالين باستخدام الصبغة الهستوكيميائية المناعية.

**النتائج:** أظهرت الجرذان المصابة بداء السكري تغيرات في النتائج البيوكيميائية والنسجية، والتي زادت في مجموعة الجنتاميسين، وأظهرت النتائج إصابة أكثر خطورة في أنابيب وكبيبات الكلى وذلك في مجموعة السكري/الجنتاميسين مع ارتفاع كبير في وظائف الكلى، وارتفاع في التعبير الجيني/البروتيني للميجالين، بالإضافة إلى زيادة التعبير المناعي لـ بي 53 و تي. ان. اف- الفا. يقلل العلاج بالسماق من الظهور المرتفع لجين وبروتين الميجالين، إلى جانب تنظيم ظهور الـ بي 53 و تي. ان. اف- الفا والحفاظ على وظائف الكلى.

**الاستنتاج:** أدى حقن الجنتاميسين في الجرذان المصابة بداء السكري المستحث بمادة السترينبتوزوتوسين إلى تلف كلوي أكثر خطورة، وقد يكون العلاج بالسماق في هذه المجموعة فعال في مواجهة هذا التلف الكلوي، عن طريق تقليل ظهور بي 53 / تي. ان. اف- الفا المعتمد على اعتراض ظهور بروتين ال. ار. بي. 2.